Comparison of charged particle identification using pulse shape discrimination and ΔE–E methods between front and rear side injection in silicon detectors

N. Le Neindre, R. Bougault, S. Barlini, Eric Bonnet, B. Borderie, G. Casini, A. Chbihi, P. Edelbruck, J.D. Frankland, Diego D. Gruyer, et al.

Comparison of charged particle identification using pulse shape discrimination and ΔE-E methods between front and rear side injection in silicon detectors.

N. Le Neindre [a] R. Bougault [a] S. Barlini [b] E. Bonnet [c]
B. Borderie [d] G. Casini [e] A. Chbihi [c] P. Edelbruck [d]
J.D. Frankland [c] D. Gruyer [c] E. Legouée [a] O. Lopez [a] P. Marini [c]
M. Pârlog [a,f] G. Pasquali [b] M. Petcu [f] M.F. Rivet [d] F. Salomon [d]
E. Vient [a] R. Alba [g] G. Baiocco [h,a] L. Bardelli [b] M. Bini [b]
R. Borcea [f] M. Bruno [h] S. Carboni [b] M. Cinausero [i] I. Cruceru [f]
M. Degerlier [i] J.A. Dueñas [j] K. Gąsior [k] F. Gramegna [i]
A. Grzeszczuk [k] M. Kamuda [ℓ] T. Kozik [ℓ] V. Kravchuk [i]
I. Lombardo [m] C. Maiolino [g] T. Marchi [i] L. Morelli [h] F. Negoita [f]
A. Olmi [e] H. Petrascu [f] S. Piantelli [e] G. Poggi [b] E. Rosato [m]
D. Santonocito [g] G. Spadaccini [m] A.A. Stefanini [b] T. Twaróg [ℓ]
M. Vigilante [m]

(FAZIA collaboration)

[a] LPC, IN2P3-CNRS, ENSICAEN et Université de Caen, F-14050 Caen-Cedex, France.

[b] INFN e Università di Firenze, via G.Sansone 1, 50019 Sesto Fiorentino (Firenze), Italy.

[c] GANIL, CEA/DSM-CNRS/IN2P3, B.P. 5027, F-14076 Caen cedex, France.

[d] Institut de Physique Nucléaire, CNRS/IN2P3, Université Paris-Sud 11, F-91406 Orsay cedex, France.

[e] INFN sezione di Firenze, via G.Sansone 1, 50019 Sesto Fiorentino (Firenze), Italy.

[f] Horia Hulubei, National Institute of Physics and Nuclear Engineering, RO-077125 Bucharest-Măgurele, Romania.

[g] INFN LNS, via S.Sofia 62, 95125 Catania, Italy.

[h] INFN e Università di Bologna, 40126 Bologna, Italy.

[i] INFN LNL Legnaro, viale dell'Università 2, 35020 Legnaro (Padova) Italy.

[j] Departamento de Fisica Aplicada, FCCEE Universidad de Huelva, 21071 Huelva, Spain

[k]*Silesian University, University of Silesia, Katowice, Poland.*

[ℓ]*Jagiellonian University, Institute of Nuclear Physics IFJ-PAN, PL-31342 Kraków, Poland.*

[m]*Dipartimento di Scienze Fisiche e Sezione INFN, Università di Napoli "Federico II", I80126 Napoli, Italy.*

Abstract

The response of silicon-silicon-CsI(Tl) telescopes, developed within the FAZIA collaboration, to fragments produced in nuclear reactions $^{84}Kr+^{120-124}Sn$ at 35 A MeV, has been used to study ion identification methods. Two techniques are considered for the identification of the nuclear products in the silicon stages. The standard ΔE-E one requires signals induced in two detection layers by ions punching through the first one. Conversely, the digital Pulse Shape Analysis (PSA) allows the identification of ions stopped in the first silicon layer. The capabilities of these two identification methods have been compared for different mountings of the silicons, i.e. rear (particles entering through the low electric field side) or front (particles entering through the high electric field side) side injection. The ΔE-E identification method gives exactly the same results in both configurations. At variance, the pulse shape discrimination is very sensitive to the detector mounting. In case of rear side injection, the identification with the "energy vs charge rise time" PSA method presents energy thresholds which are significantly lower than in the case of front side injection.

Key words: Pulse shape discrimination, ΔE-E, Silicon detector, Charge signal, Current signal
PACS: 29.30.Ep, 29.30.-h, 29.40.-n, 29.40.Wk, 84.30.Sk

1 Introduction

The goal for the next generation of nuclear physics experiments will be to take maximum advantage of the increasing number of radioactive heavy-ion beams delivered by the existing and planned accelerator facilities. The nuclear structure as well as the thermodynamics and dynamics of excited exotic nuclei far from the stability valley can be studied. In particular, for the equation of state of nuclear matter it will be possible to explore the temperature and density dependence of the symmetry energy term on isospin. The aim of the FAZIA collaboration [1] is the definition and construction of a detector system for this purpose. A high granularity and large acceptance 4π apparatus for a detailed study of heavy-ion collisions in a wide range of bombarding energies (from a few to about 50 A MeV) is planned. In order to study the isospin degree of

2

freedom, it is very important to extend as far as possible the isotopic identification capabilities of the detectors towards heavy fragments while keeping the energy thresholds very low. With this objective, few years ago the FAZIA collaboration started an R&D program, based on the optimization of the performances of three-layers Si-Si-CsI telescopes and sizeable improvements have been obtained for both the standard ΔE-E technique and the Pulse Shape Analysis [2] (hereafter PSA) in each of the silicon stages. Most efforts have been spent on the latter for ions which are stopped in the first Si-layer and cannot be identified via the ΔE-E method. Indeed, because of the different stopping powers, different particles with the same kinetic energy, or the same velocity, produce different energy loss profiles along the detector depth and this results in different charge collection times, i.e. in different pulse shapes [3]. Both techniques, and in particular the PSA, have benefited from the digital signal processing made possible by a new digital sampling electronics [4], [5], [6]. Other groups [2], [7], [8], [9], [10], [11], [12], [13], [14], [15], [16] have also investigated the behaviour of silicon detectors for PSA applications in previous years.

The aim of the present paper is to compare PSA techniques for two different particle injection. Indeed, the shape of the signals produced by particles crossing a semiconductor detector is very sensitive to the strength and the configuration of the electric field F(x) inside the detector. Therefore, as expected, we have observed a different behaviour when nuclear products enter the silicon np junction through the front side with the high electric field or through the rear side with the low electric field [17]. For a specified ion, the shape (as a function of time) of the induced signal depends, besides the specific rate of energy loss and the electric field, on the detector capacitance and preamplifier characteristics. Using exactly the same detector and preamplifier for particle incidence on the front or on the rear side should provide a better understanding of the signal shapes [17]. In literature both configurations have been successfully tested [2], [6], [9], but even when both mountings were used (e.g. in [2]) they have not been compared for the same detector and electronics. The front configuration presents a priori a big advantage if one wants to perform, besides the pulse shape, a Time of Flight (ToF) measurement, since the signals are faster. But the gain in ToF identification can imply a spoiling of PSA and a compromise should be found. In this experiment for the first time the very same detectors, preamplifiers, applied voltages and electronics have been used for both settings, allowing a fair comparison exactly in the same conditions, including reaction product distributions. PSA correlations and their qualities in terms of energy thresholds and shapes will be investigated.

3

2 Experimental setup

A 35 A MeV ^{84}Kr beam, delivered by the "Ciclotrone Superconduttore"(CS) of the "Laboratori Nazionali del Sud" (LNS) in Catania, was used for bombarding thin targets of ^{124}Sn, ^{120}Sn, ^{112}Sn, and ^{nat}Au. All results presented in this paper refer to the reaction products obtained by adding up the data of those reactions, in order to obtain larger statistics.

Table 1

Properties of the silicon detectors, CsI(Tl) and electronics used for ΔE-E and pulse shape measurements.

Technical specifications	Si1	Si2	CsI
Manufacturer	FBK	FBK	Amcrys
Bulk type	n	n	
Thickness	300 μm	500 μm	10 cm+FBK photodiode
Depletion voltage	132 V	290 V	
Applied voltage	140 V	260 V	30 V
Resistivity unif.(FWHM)	$\simeq$4%	-	
Digitizer (bit/rate)	14 bit/100 MHz	14 bit/100 MHz	12 bit/125 MHz
Exp. full Range	$\geq$3 GeV	$\simeq$2 GeV	$\simeq$0.4 GeV

2.1 Telescope mounting

In this experiment we used the same telescope configuration as the one foreseen for the future FAZIA 4π array. The telescope composed of Si 300 μm-Si 500 μm-CsI(Tl) 10 cm, was mounted in the "Ciclope" scattering chamber at LNS, at a distance from target of $\simeq$1 m and at $\simeq$5.4^o polar angle with respect to the beam line, slightly beyond the grazing angles, i.e. the scattering angles corresponding to very peripheral projectile-target nuclear collisions, where the reactions mechanism concentrates the largest variety of products. Conversely to a previous experiment [6] a CsI detector was added to reject particles punching through the second silicon Si2. Some characteristics of the telescope and of its dedicated electronics are given in Table 1.

2.2 Properties of the detectors and their electronics

The silicon detectors come from random cut wafers. They are ion-implanted, of the neutron transmutation doped (n-TD) type, with bulk resistivity values

in the range 3000-4000 Ωcm and an active area of 20×20 mm^2. They were manufactured by FBK (Trento, Italy) in transmission mounting, with dead layers on both sides of $\simeq$500-800 nm to improve their robustness. The 10 cm long CsI crystal is produced by Amcrys. Its lateral surfaces have been wrapped with the new Vikuiti^{TM} ESR 3M reflecting polymer, while its back square face has been glued to a custom design photodiode produced by FBK.

Each element of the FAZIA telescopes (silicon detectors and CsI scintillators) was coupled to custom-built Front End Electronics (FEE), consisting of a charge-and-current preamplifier (PACI: Pre-Amplifier for Charge and I-current) [18] followed by sampling ADCs (digitizers). The preamplifiers had different gains and were located near the detectors, inside the vacuum chamber. The digitizers were in air, connected to the preamplifiers by differential cables. They were either 125 MS/s 12 bit cards for CsI [19] ("Florence cards" developed by INFN-Sezione di Firenze) or 100 MS/s 14 bit cards for silicons (developed by IPNO-Orsay, in the framework of the FAZIA collaboration). The sampled waveforms delivered by the digitizers were then stored on disk and processed off-line in order to extract the relevant quantities for the analysis. The improvements in the identification capabilities presented in this paper are the result of several procedures which were developed during the R&D preparatory phase, see [4], [5], [6], [20], [21] and [22].

2.3 Identification techniques

The ΔE-E technique is based on the measurement of the energies deposited by the impinging particle in two detectors after punching through the first layer. The PSA, on the other hand, requires the energy measurement of the reaction products stopped inside one detector and an additional parameter related to the shape of the charge signal or of the current signal [6]. In the present paper, this shape-related parameter is either the rise time of the charge signal for the "Energy vs Charge rise time" method, or the maximum of the current signal (called amplitude max in [22]) for the "Energy vs Current maximum" method. The algorithms and techniques for the digital signal processing employed in this analysis are described in [4] and [5]. Energy measurements as in [6].

During the first part of the experiment, particles impinged on the detectors through the high electric field side (front side injection) for both silicons (Si1 and Si2) of the telescope. Then for the second half of the experiment, we turned both the Si1 and Si2 by 180° in order to compare the front and rear side injection configurations in the same conditions regarding detector characteristics, depletion voltages and electronics.

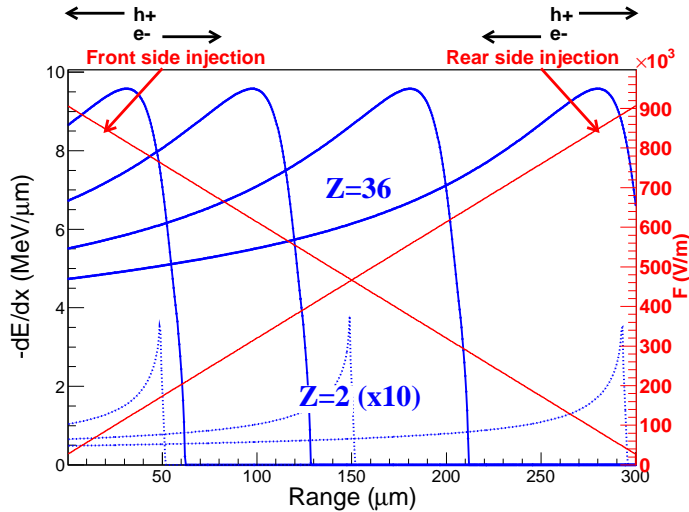## 3   Rear or Front side particle injection?

Fig. 1. *For the first silicon (Si1 of table 1), electric field (red lines) in V/m (red right scale) as a function of the depth for the two different mountings: front and rear side injection; particles enter from the left in both cases. The calculated energy losses [23], [24], [25] as a function of the range of the stopped particle in the semiconductor are also indicated in MeV/μm (black left scale) for alpha particles (for 2, 4 and 6 A MeV and they have been multiplied by a factor of 10 to scale the figure) and a ^{84}Kr nucleus (for 6, 12, 18 and 24 A MeV).*

The time dependence of the current signal in semiconductors is ruled essentially by two phenomena: the charge carrier dissociation (the plasma erosion time) and the duration of the drift of the electrons (e$^-$) and holes (h$^+$) towards the appropriate electrodes, which depends on electric field strength and carrier mobilities. The plasma erosion time is longer for higher densities of charge carriers along the incident ion ionization track, as it happens for higher atomic number Z. It depends also on the local electric field strength which varies with the injection side and penetration depth (see Fig. 1). For what concerns the charge carrier drift time, for a stopped particle in the first microns of the semiconductor (short track), in the rear side injection case, the electrons and holes experience first the low electric field. In particular the holes, which move towards opposite side (see Fig. 1), and have a mobility almost three times lower than the electrons, have to cross a major part of the thickness, thus increasing the collection time. In the front side injection case, for short tracks, particles stopped in the first few microns, the slower charge carriers (the holes) are collected by the close entrance side (front side) and their path lengths are shorter, thus reducing their collection time.

At variance, for particles almost punching through the silicon layer (long tracks), the Bragg peak, responsible for the maximum density of charge carriers, stands near the exit side of the detector. So in the rear side injection case most of the charge carriers (those in the Bragg peak) "feel" a high electric

field that strongly reduces the plasma erosion time. In the front side injection case the maximum density of charge carriers is located in the low electric field, thus plasma erosion time gets longer and signal rise times increase.
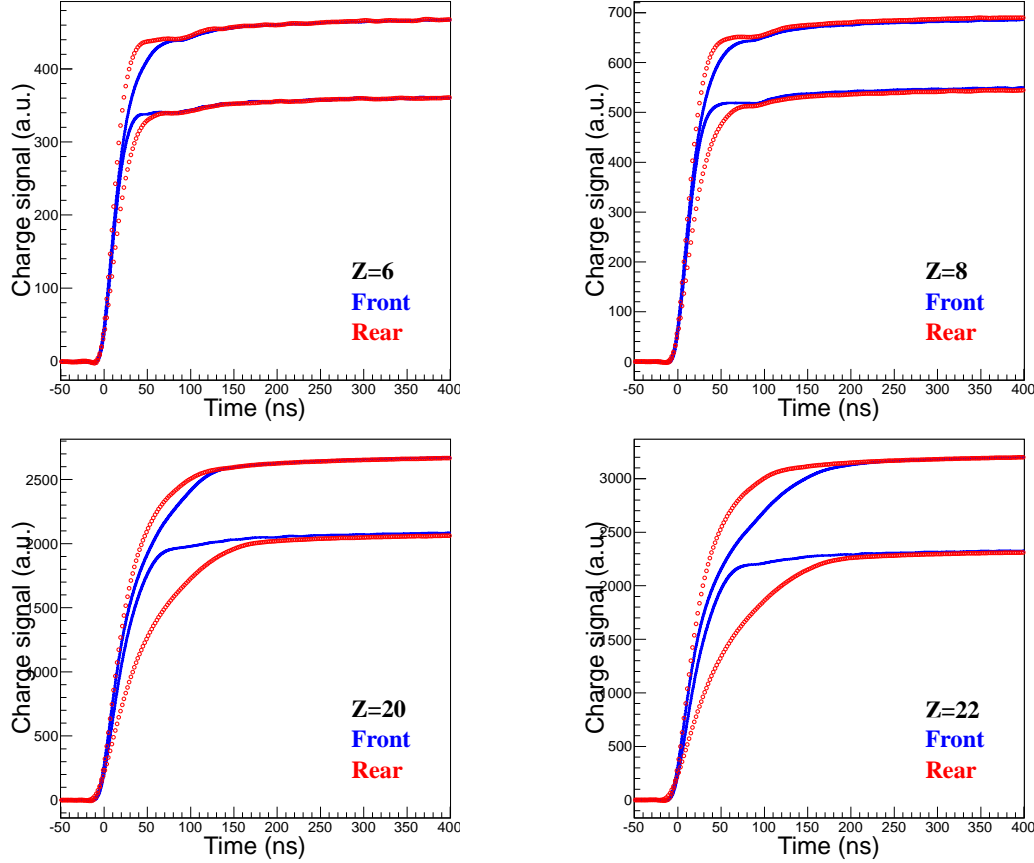

Fig. 2. *Comparison between mean charge signal shape in front (blue full lines) and rear (red dotted lines) side injection for various particles of two energies (ranges) stopped in the silicon: Z=6: 105 MeV (203 μm) and 130 MeV (286 μm), Z=8: 160 MeV (197 μm) and 200 MeV (282 μm), Z=20: 590 MeV (185 μm) and 760 MeV (267 μm), Z=22: 660 MeV (182 μm) and 910 MeV (289 μm), respectively. In each panel, the higher plateau charges (blue full lines and red dotted lines) correspond to the higher energy value (see text for explanation).*

This point is illustrated in Fig. 2 where charge signals for several nuclei stopped in the first silicon (Si1), at two different energies are shown in front (blue full lines) and rear (red dotted lines) side injection. The higher energy (larger signal amplitudes) corresponds to particles almost stopped at the end of the detector, whereas the low one refers to nuclei stopping just after the middle of the detector. We first observe that, at a given energy, the amplitude of the signal is independent of the entrance side. For particles almost punching through the first silicon junction, the signal shapes have a shorter rise time when the particles enter through the low electric field side (red dotted lines signal shapes of higher amplitude in each panel of Fig. 2. For nuclei stopped

in the middle of the silicon layer (lower signals) the trend is opposite: rear side injection produces longer signal rise times. We recall that we are comparing results obtained with exactly the same detector and electronics. When the shape is used for discrimination, one may think that a larger signal shape variation would improve particle identification. Therefore, based on the shapes shown in Fig. 2, it intuitively appears that rear side injection will be, a priori, more favourable for PSA; it shows a larger variety of signal shapes and larger variations of the charge collection time.

Indeed in our previous experiment [6], as in other works [2], [7], [8], [10], [11], [12], ion discrimination was performed for particles entering the low electric field. We will now quantify the differences between the two mountings, by comparing the PSA performances (in terms of quality and energy thresholds) for rear and front side injection, using the two "Energy vs Charge rise time" and "Energy vs Current maximum" methods already used in the literature [2], [6], [10], [16]. However, we first want to explore the consequences of the silicon mounting on the ΔE-E identification technique (indeed it is mandatory to preserve first the excellent ΔE-E identification capabilities of the FAZIA detectors). So, in the next section, we will compare the ΔE-E performances for the two configurations. We expect, once the charge carriers are all collected and the signals properly filtered, both configurations to give the same quality of energy information: indeed, at variance with PSA, the ΔE-E method does not exploit the time development of the signals within the silicon.

4 Identification of fragments with ΔE(Si1)-E(Si2) method

In this section the performances of the ΔE-E method are compared in both configurations (rear and front side injection). In each silicon stage, the energy deposited is extracted from the total collected charge. We can see from Fig. 3 that, apart the slight difference due to the use of different targets (and thus slightly different cross sections for the production of elements), we obtain comparable identification maps in both cases, demonstrating the same quality of the energy measurement. A zoom at low energy for light nuclei, shown in Fig. 4, confirms the equally good isotopic identification at least for elements from H to Ti.

A more quantitative comparison is made in Fig. 5, where the previous maps have been linearized in order to get the Particle IDentification (PID) number distribution from neon to argon isotopes (similar results have been obtained for Z=1-9). Please note the logarithmic scale on the ordinate axis. The Gaussian isotopic distributions are completely separated at the level of their full width at half maximum height (FWHM), i.e. their FWHM never overlap for two adjacent isotopes. The quality of the isotopic separation is identical for front
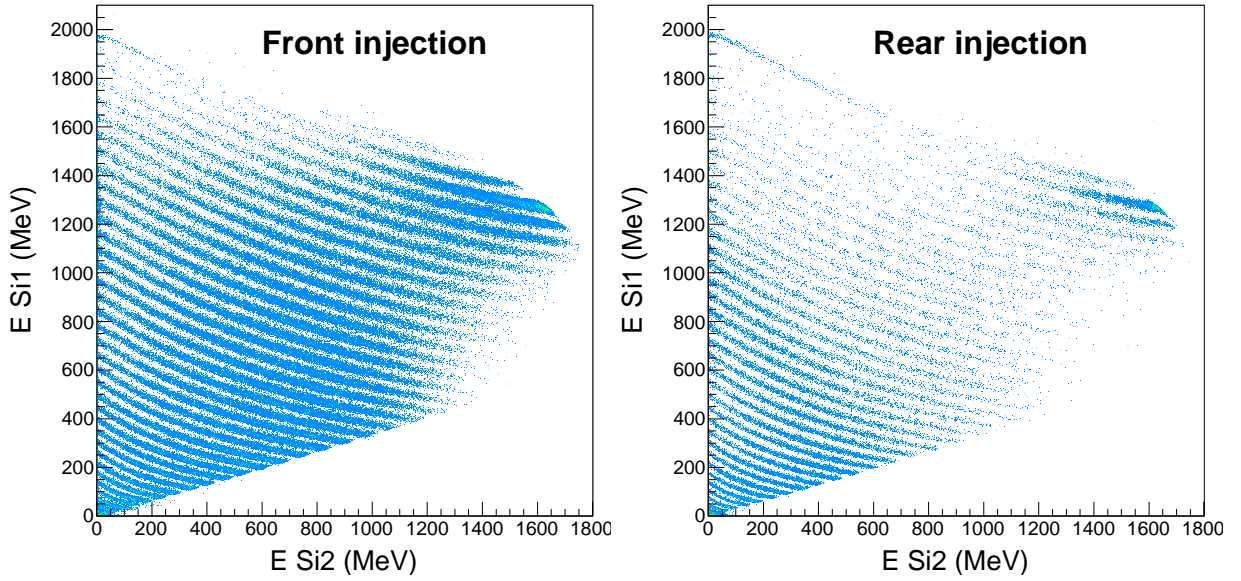
8

Fig. 3. *ΔE(Si1)-E(Si2) matrices for front (left panel) and rear (right panel) side injection. Particles punching through the second detector have been removed via a veto on the CsI signals.*
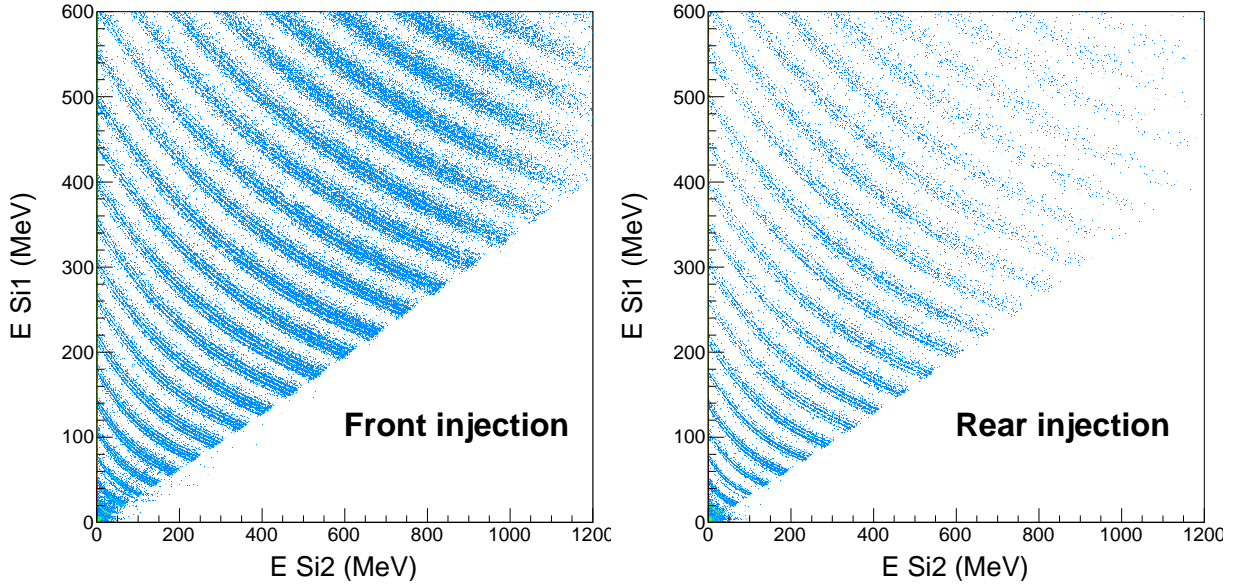

Fig. 4. *Expansion of the low energy parts of Fig. 3 showing the obtained isotopic resolution. Particles punching through the second detector have been removed via a veto on the CsI signals.*

or rear injection, proving that for the ΔE-E method the energy measurement remains quantitatively the same, independent of the injection side. The only difference one may expect concerns the recombination of charge carriers along the track, contributing to Pulse Height Defect (PHD) phenomena that are quite important in the case of passivated ion-implanted silicon detectors [26]. Recombination leads to a loss in the collection of electrons and holes (and
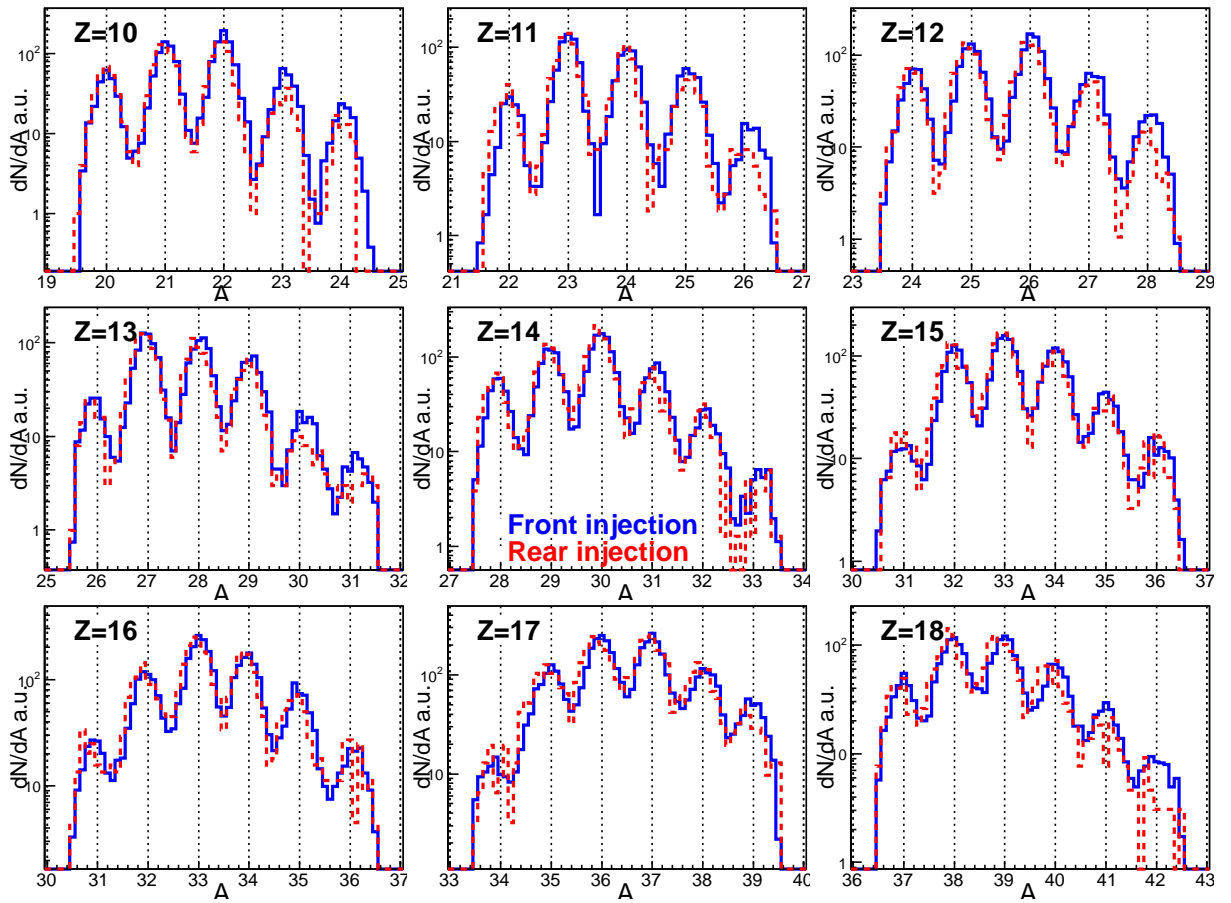
Fig. 5. *Linearization of the previous $\Delta E(Si1)$-$E(Si2)$ matrices, see Fig. 4, for both configurations, front (blue full line) and rear (red dashed line) side injection. For each atomic number Z, isotopic spectra have been normalized on the yields obtained for ^{21}Ne, ^{23}Na, ^{25}Mg, ^{27}Al, ^{29}Si, ^{32}P, ^{32}S, ^{35}Cl and ^{38}Ar respectively*

thus to a reduction of the measured energy) that is favoured by high charge densities and/or by a low electric field. Therefore this effect may depend on the injection side. The similarity of energy values measured for the two injection modes suggests that recombination is very small for the n-TD type detectors.

5 Comparison of Pulse Shape Analysis (PSA) in silicon for different injection modes

The PSA allows to identify particles stopped in one silicon detector from the information delivered by that detector only (Si1, 300 μm). Therefore, all results presented in this section have been obtained with a veto condition on the detector behind (Si2, 500 μm). The two methods of PSA used here, "Energy vs Charge rise time" and "Energy vs Current maximum", have been both successfully used by the FAZIA group and others, see [6], [16]. In order to

have large dynamic ranges ($\simeq$2-3 GeV), low amplification values were used in the present experiment. A consequence of this choice was that no isotopic resolution with PSA could be observed, at variance with other FAZIA experiments using higher amplifications. Consequently the identification thresholds and Figure of Merit (FoM) [5], [6] calculated hereafter for PSA refer only to charge discrimination and are meant, in particular, to compare the two opposite injection faces.
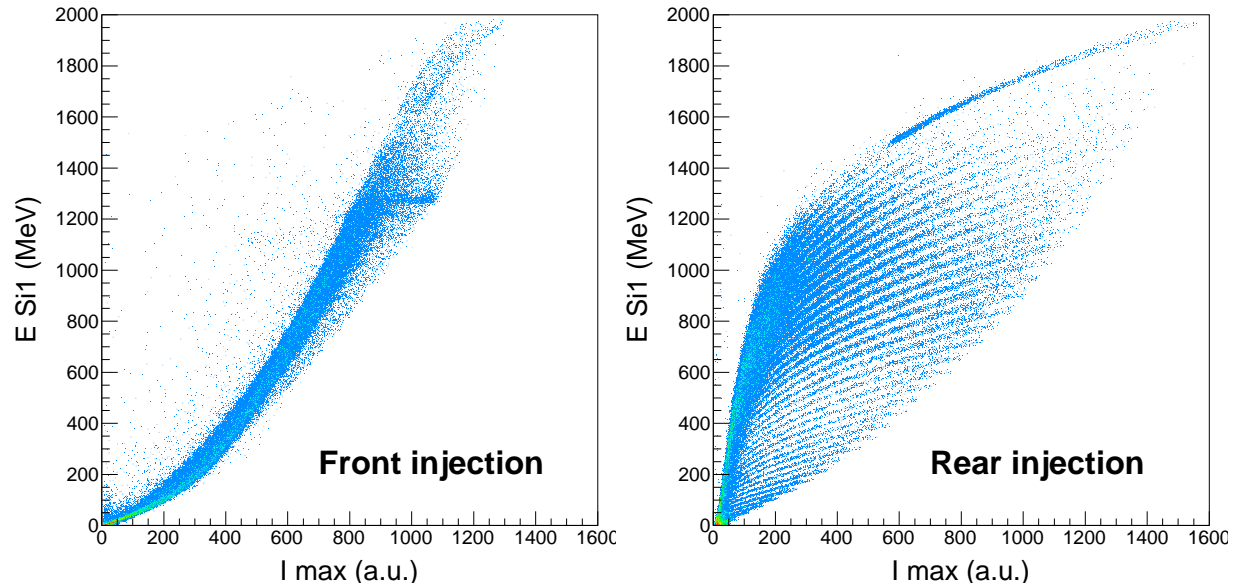

Fig. 6. *Energy vs maximum amplitude of the current signal Imax for particles stopped in the first silicon (Si1). Particles punching through the detector have been removed.*

5.1 PSA by energy vs maximum amplitude of the current signal

Figure 6 shows the "Energy vs Current maximum" correlation for both cases, front side injection (on the left) and rear side injection (on the right). For the rear side injection, we recover the identification map previously studied in the framework of the FAZIA collaboration, see [4], [5], [6]. The populated ridges allow to identify all atomic numbers from Z=1 to 36 (Kr beam). On the contrary, in the front side injection configuration no identification is visible. All elements merge together in a very compact cloud, corresponding to a strong correlation between the energy and the maximum current. Thus the maximum amplitude of the current signal is not a good PSA variable when the fragments enter through the high electric field side. We recall that only particles stopped in the first silicon of the telescope have been kept, the particles punching through have been removed.
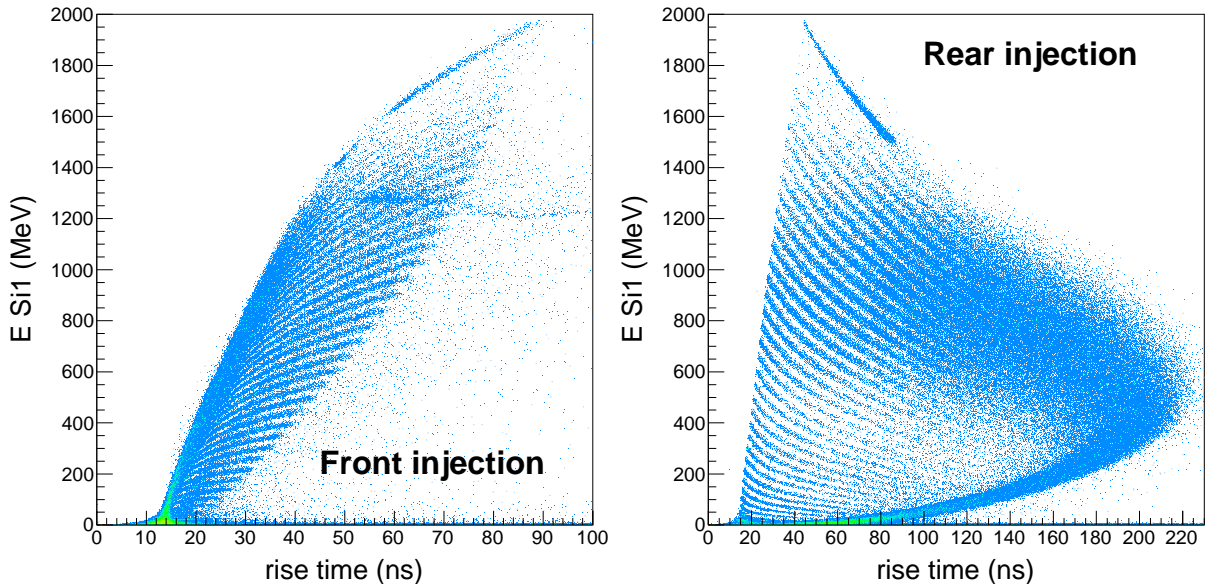
11

Fig. 7. *Energy vs rise time of the charge signal for particles stopped in the first silicon (Si1). Particles punching through the detector have been removed.*

5.2   PSA by energy vs rise time of the charge signal

Regarding the energy vs rise time of the charge signal shown in Fig. 7, we obtain in both cases identification maps similar to those presented in [5], [6] (for rear side injection) and [10] (for front side injection). As previously mentioned, we observe a very large increase of the maximum measured rise time (almost a factor of two, $\simeq$200 ns instead of $\simeq$100 ns) for the rear side injection configuration. Moreover, the shape of the correlation between energy and charge rise time is very different in the two cases. In the front side injection, the charge rise time continuously decreases with decreasing ion energy for all Z values. On the contrary, for rear side injection, starting from high kinetic energies, we observe a rise-and-fall trend of the rise time which, for slow ions, produces a ridge where all values merge together, whatever the particle is. In both cases a "no identification" zone is visible for each line at low energy, defining a Z dependent identification threshold. These thresholds will be determined more precisely in the following.

In Fig. 8 we present the same PSA matrices as in Fig. 7 but without removing the punching through particles, i.e. including particles which pass through Si1 and are stopped either in the second silicon or in the CsI. This presentation may be interesting because in some cases one might be tempted to apply the PSA in simply one silicon layer, without a veto on the second stage detector. This is the case of tagging systems mounted along the transport line of radioactive beams produced in fragmentation. The lack of a second layer qualitatively results in the spoiled correlations energy vs rise time of Fig. 8 (in our case most of the punching through ions are in the region of the Kr
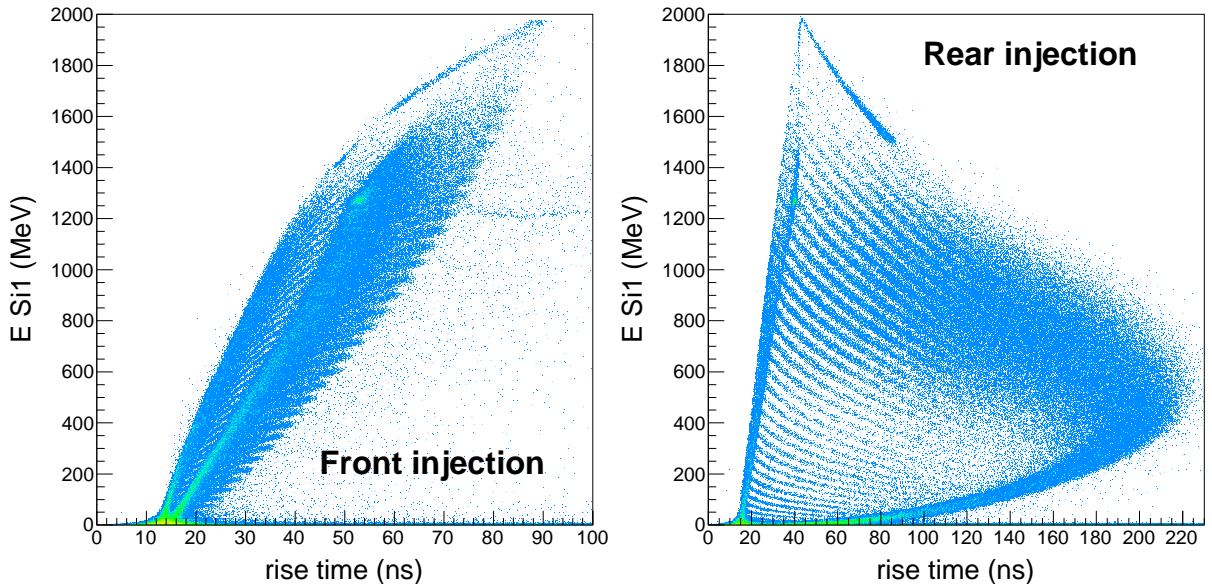
12

Fig. 8. *Energy vs rise time of the charge signal in the first silicon (Si1). Same as Fig. 7 but in this case punching through events have not been removed.*

projectiles). From Fig. 8 one sees that in the rear side injection case punching through particles are located on the very left part of the identification matrix. They are superposed on a rather narrow strip of high-energy stopped particles. Therefore, they introduce a threshold in the high energy zone of the PSA identification capability, but most of the PSA matrix is free from such a contamination. On the contrary, in the front side injection case, punching through particles lie just in the middle of the PSA matrix thus severely spoiling the identification. This constitutes a very strong limitation.

5.3 Particle identification thresholds for rear and front configuration

The PSA method based on "Energy vs Current maximum", does not allow to identify particles in the front side injection configuration. Therefore a comparison between front and rear side injection can be performed only on the basis of the second PSA technique, namely the "Energy vs Charge rise time" one. In this case, for the same stopped products, Fig. 7 shows very different identification maps. Even though the rear side injection method may seem more efficient, since it enlarges the ridges range, we need a more quantitative way to judge the identification quality for both configurations. Therefore we applied the same protocol as in [6]. A Figure of Merit (FoM) defined as

$$FoM = \frac{|\overline{PID2} - \overline{PID1}|}{FWHM1 + FWHM2}$$

was determined for adjacent Z as a function of the energy. Here FWHM1,2 are the full widths at half maximum of the Gaussian distributions of two

13

adjacent elements of atomic number Z, Z+1. The corresponding PID1,2 stand for the peak values of the linearized ridges, as those obtained in case of the ΔE-E method in Fig. 5 for isotopic distributions. A value of FoM=0.7 was conventionally chosen in order to extract a low energy threshold above which we realize a good identification. A FoM value of 0.7 corresponds, for two peaks of equal intensity, to a peak-to-valley ratio of 2.0, see [5]. The same value FoM=0.7 leads to different energy thresholds of identification for different adjacent ejectiles. The method was applied to both matrices of Fig. 7. The identification thresholds are summarized in Fig. 9 in terms of energy (left) and energy per nucleon (right) using, for ions heavier than Z$\geq$6, the mass parameterization A=2.08$\times$Z+0.0029$\times$Z^2. As in [6], we have reported also the energy thresholds obtained with the standard ΔE-E technique (black symbols and line) inherently introduced by the first 300 μm thick silicon detector. One may clearly see a spectacular improvement on the identification energy threshold for the rear side injection technique (red symbols and line). For example, a gain of almost a factor of two in energy per nucleon is achieved for Z$\simeq$10-15. The thresholds obtained in the front side injection case are very similar to those published in [10] for other silicon junctions, indicating that they do not depend on the detector. At variance the corresponding rise time depends on the detector thickness and the applied voltage (electric field).
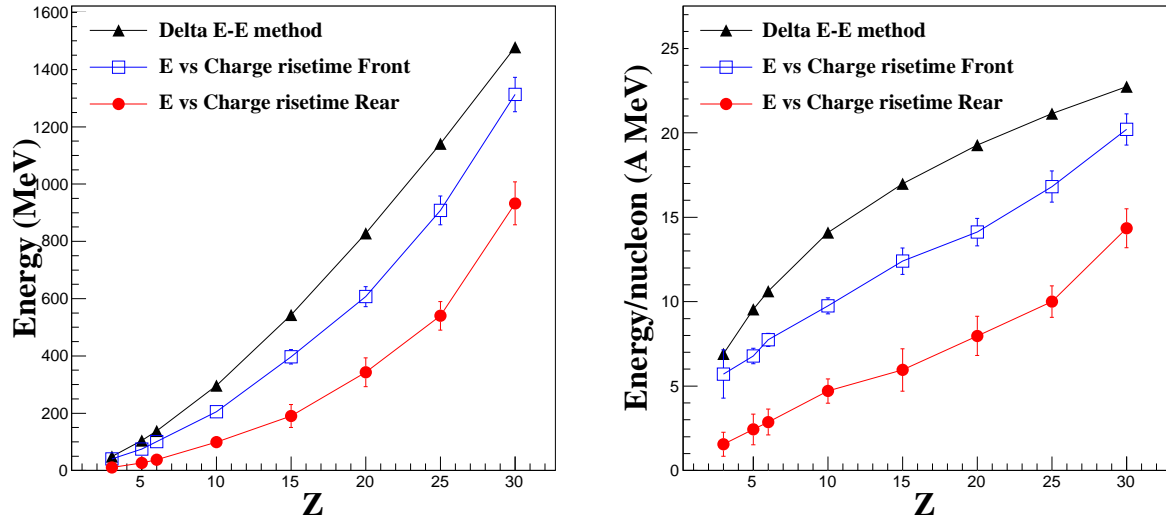

Fig. 9. *Energy thresholds for Z identification with ΔE(300 μm)-E technique (black triangles) and with PSA technique (energy vs charge rise time: red points "rear side injection" and blue squares "front side injection") as a function of atomic number Z. The thresholds values are presented in terms of total energy (left) and energy per nucleon (right). Error bars take into account the statistic and the FoM method reproducibily to extract the energy thresholds.*

Expressed as a function of the range in silicon, see Fig. 10, the threshold differences are even more impressive. In the front side injection case the mini-
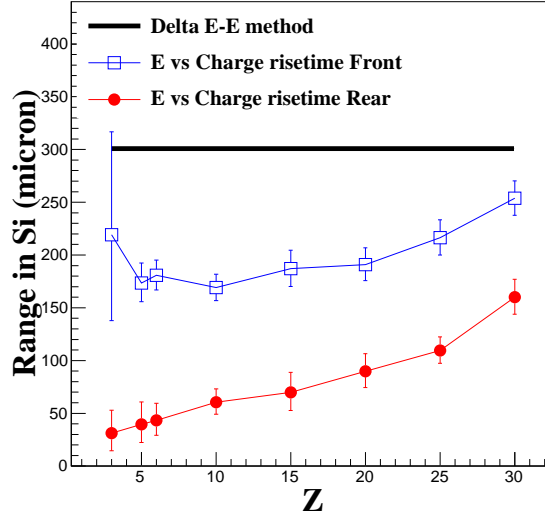
14

Fig. 10. *Thresholds expressed in term of range in silicon material for Z identification with ΔE(300 μm)-E technique (black triangles) and with PSA technique (energy vs charge rise time: red points "rear side injection" and blue squares "front side injection") as a function of atomic number Z. Error bars take into account the statistic and the FoM method reproducibility to extract the energy thresholds.*

mum range for identification exhibits a concave shape with thresholds always larger than 150 μm, whereas in the rear side injection case the minimum range presents a continuous increase, from 30 to 160 μm. As already mentioned in [6] these thresholds do not depend on the detector thickness but it rather seems that they are a characteristic of reverse polarized silicon junctions [27]. Comparing the present results to those of [6], it also appears that the Z-identification thresholds increase with the bulk resistivity inhomogeneity.

6 Conclusions

In this experiment we have carefully compared the results of the digital "Pulse Shape Analysis"(PSA) technique for identifying stopped reaction products in a n-TD silicon detector for two different configurations: one in which the particles enter from the high electric field side (front side injection) and the other for incidence on the low electric field side (rear side injection). Two PSA techniques, previously successfully tested in the rear configuration, were examined. One, here called "Energy vs Current maximum", completely fails in the front side injection mode at variance with the rear side injection one. The other, "Energy vs Charge rise time", gives a very satisfactory result in both cases: full charge separation is obtained up to the maximum observed Z=36. However, in this latter case, the energy identification thresholds of atomic

15

number Z are very different, with higher values for particles entering from the high electric field side. Among the two examined configurations, the present analysis indicates that the rear side injection mode has to be chosen for a better ion identification.

References

[1] Web site Fazia collaboration (http://fazia.in2p3.fr/spip/)

[2] G. Pausch et al., NIMA 322 (1992) 43

[3] H. Hamrita et al., NIMA 642 (2011) 59

[4] L. Bardelli et al., NIMA 521 (2004) 480

[5] L. Bardelli et al., NIMA 654 (2011) 272

[6] S.Carboni et al., NIMA 664 (2012) 251

[7] G. Pausch et al., NIMA 337 (1994) 573

[8] G. Prete et al., NIMA 442 (1999) 263

[9] K.W. Lee et al., Journal of the Korean Physical Society, vol.53, n^o2 (2008) 1197

[10] M. Alderighi et al., IEEE Transaction on Nuclear Science vol.53, n^o1 (2006) 279

[11] F. Amorini et al., IEEE Nuclear Science Symposium Conference Record N36-4, (2009) 2115

[12] M. Mutterer et al., NIMA 608 (2009) 275

[13] B. John et al., NIMA 609 (2009) 24

[14] Yongming Li et al., NIMA 625 (2011) 35

[15] M. von Schmid et al., NIMA 629 (2011) 197

[16] J.A. Dueñas et al., NIMA 676 (2012) 70

[17] M. Parlog et al., NIMA 613 (2010) 290

[18] H. Hamrita et al., NIMA 531 (2004) 607

[19] G. Pasquali et al., NIMA 570 (2007) 126

[20] L. Bardelli et al., NIMA 602 (2009) 501

[21] L. Bardelli et al., NIMA 605 (2009) 353

[22] S. Barlini et al., NIMA 600 (2009) 644

[23] L.C. Northcliffe, R.F. Schilling, Atomic Data and Nuclear Data Tables A 7 (1970) 233

[24] F. Hubert, R. Bimbot, H. Gauvin, Atomic Data and Nuclear Data Tables 46 (1990) 1

[25] E. De Filippo rapport Dapnia-SphN-95-60, 1995

[26] G. Tabacaru et al., NIMA 428 (1999) 379

[27] FAZIA collaboration, paper in preparation